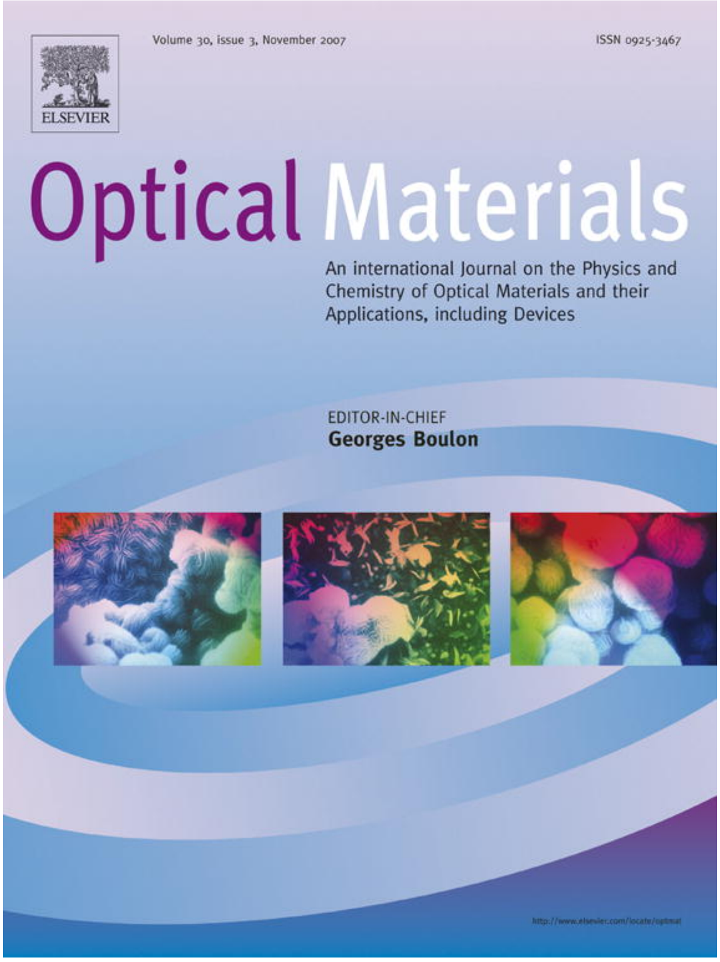
Volume 30, issue 3, November 2007
ISSN 0925-3467
ELSEVIER
Optical Materials
An international Journal on the Physics and Chemistry of Optical Materials and their Applications, including Devices
EDITOR-IN-CHIEF
Georges Boulon
http://www.elsevier.com/locate/optmat

Available online at www.sciencedirect.com

ScienceDirect

Optical Materials 30 (2007) 478–485

www.elsevier.com/locate/optmat

Optical characterization of amorphous oligo(4,4′-biphenylene-1,1-substituted methylene)s

Pablo G. Del Rosso [a], Marcela F. Almassio [a], Silvia S. Antollini [b], Raúl O. Garay [a,*]

[a] *Instituto de Investigaciones en Química Orgánica, Universidad Nacional del Sur, Avenida Alem 1253, 8000 Bahía Blanca, Argentina*
[b] *Instituto de Investigaciones Bioquimicas de Bahia Blanca, Camino La Carrindanga Km 7 – C.C. 857, 8000 Bahía Blanca, Argentina*

Received 22 November 2006; received in revised form 20 December 2006; accepted 14 January 2007
Available online 27 February 2007

Abstract

Oligo(*p*-biphenylene-1,1-substituted methylene)s with *p*-biphenylene units tethered along the oligomer main chain by their para positions to isopropylene, perfluoroisopropylene, cyclohexylene or fluorenylene spacers were synthesised from dimesylates using the Ni homocoupling reaction. GPC, NMR, DSC and POM techniques showed that they are amorphous with high T_g and have low polydispersity indexes, few residual end groups and good solubilities. The materials are UV-absorbers and emitters with good film-forming properties. The increase in size or polarity of the isopropylidene spacer does not bring major changes in their optical properties while the introduction of a fluorene spacer substantially modifies its optical response. Their absorption and emission behavior indicated that the spacers isolate the gem-biphenyls and the small differences observed in absorption maxima can be assigned to substitution effects instead of homoconjugative effects. No aggregate formation was detected by red-edge excitation experiments indicating that their contorted chain conformations hinder interactions between the biphenylene chromophores although the fluorenylene-spaced oligomer form fluorene excimers. Fluorescence anisotropy indicated that all these disordered cromophoric assemblies have high bulk exciton mobilities. The propylidene-spaced oligomer is very efficient as a donor for energy transfer.

Keywords: Segmented conjugated polymers; Amorphous; Luminescence; Biphenyl; Synthesis

1. Introduction

Poly(*p*-arylene alkylene)s, that could be considered regularly segmented conjugated polymers [1], are a rather unknown polymer class [2], although poly(*p*-xylylene)s are the exception since they have been used for many years as protective coatings [3,4], application that has been recently extended to organic light emitting diodes [5]. Presently, another family, the poly(*p*-biphenylene methylene)s, is being considered as a candidate for bistable memory devices [6]. All these polymers have hydrophobic character, excellent thermal properties and the members with even number of methylenes are highly crystalline. Thus, poly(*p*-arylene alkylene)s have inherently limited solubilities, mainly as a result of the absence in their structure of functional groups which can establish favourable enthalpic interactions with solvents precluding wet processability. However, when the alkylene spacer consists of a single saturated carbon atom the polymer main chain is forced to adopt folded conformations that yield amorphous phases and improve solubility at the expense of increased gas permeability. Regrettably, polymer processability is much reduced as the size of the alkylene moiety dwindles or the size of the aromatic moiety increases [2]. Thus, oligomeric samples of poly(*p*-biphenylene methylene)s are sparingly soluble in common organic solvents [6]. Interestingly, Sheares demonstrated that substitution of the methylene spacer by a perfluorinated isopropylidene spacer in poly(*p*-biphenylene methylene)s markedly increases polymer solubility [7].

Indeed, poly(*p*-biphenylene methylene)s are very stable wide-band-gap materials whose low intrinsic electrical

---

[*] Corresponding author. Tel.: +54 291 4595101; fax: +54 291 4595187.
E-mail address: rgaray@criba.edu.ar (R.O. Garay).

0925-3467/$ - see front matter © 2007 Elsevier B.V. All rights reserved.
doi:10.1016/j.optmat.2007.01.007

conduction is generating interest but less is known regarding the optical properties of these disordered assemblies of biphenylene chromophores. As more attention is paid to materials and devices optically active in the ultraviolet region, biphenylenes could play a role in high-resolution optical data storage and photolithography [8]. Therefore, in order to investigate the influence of structural modifications in the saturated spacer on the optical behaviour of poly(*p*-biphenylene methylene)s we synthesized a series of oligomers with markedly different spacer structure. The oligomeric state ensured processability while in principle the optical properties of these materials should be to great extent independent of the chain length due to its segmented nature. The optical properties were investigated using UV–visible absorption and steady-state photoluminescence emission and fluorescence anisotropy.

2. Experimental

2.1. Materials

Reagents and solvents were purchased from Aldrich and used without further purification unless otherwise specified. Bistriphenylphosphine nickel dichloride was prepared as described in the literature [9] THF was purified by distillation from Na/benzophenone.

2.2. Monomer and oligomer synthesis

2.2.1. 2,2-Bis-(4-[(methylsulfonyl)oxy]phenyl)propane (2a)

The general procedure used for the synthesis of monomers **2a–d** is described in detail for 9f. To a solution of bisphenol A (2.31 g, 10.0 mmol) and TEA (3.04 g, 30.0 mmol, 4.39 mL) in CH_2Cl_2 (50 mL) at 0 °C under nitrogen atmosphere was added drop wise mesyl chloride (2.62 g, 23.0 mmol, 1.8 mL) and then stirred during half an hour. The mixture was washed with ice water (30 mL), 5% aqueous HCl (30 mL), 5% aqueous Na_2CO_3 (30 mL), brine (30 mL) and ice water (2 × 30 mL), dried with Na_2SO_4. The solvent was removed under reduced pressure. The solid was treated with hexane (60 mL) for 1 h, filtered and dried in vacuo. Yield: 3.52 g, 91 %. m.p. = 97–99 °C. The numbering system showed in Fig. 2 to describe the proton and carbons in the range of structurally similar compounds was applied to the ^1H and ^{13}C NMR spectra. ^1H NMR ($CDCl_3$): 7.22 (m, 4 $H^{5,6,8,9}$), 3.15 (s, $3H^3$), 1.68 (s, $3H^1$). ^{13}C NMR: 149.6 (C^7), 147.1 (C^4), 128.1 ($C^{5,9}$), 121.3 ($C^{6,8}$), 42,4 (C^2), 37.1 (C^3), 30.6 (C^1).

2.2.2. 2,2-Bis-(4- [(methylsulfonyl)oxy]phenyl)-perfluropropane (2b)

This was synthesized from 2,2-bis-(4-hydroxyphenyl)perfluropropane. Yield: 4.75 g, 96 %, m.p. = 136–137 °C. ^1H NMR ($CDCl_3$): 7.37 (m, $4H^{5,6,8,9}$), 3.20 (s, $3H^3$). ^{13}C NMR: 149.6 (C^7), 132.0 ($C^{5,9}$), 123.9 (c, $^1J_{C-F}$ 287.0) (C^1), 22.0 ($C^{6,8}$), 64.1 (m, $^2J_{C-F}$ 25.8) (C^2), 37.9 (C^3).

2.2.3. 1,1-Bis-(4-[(methylsulfonyl)oxy]phenyl) cyclohexane (2c)

This was synthesized from bis-(4-hydroxyphenyl)ciclohexane. Yield: 3.9 g; 91%, m.p. = 114–115 °C. ^1H NMR ($CDCl_3$): 7.24 (m, $4H^{5,6,8,9}$), 3.11 (s, $3H^3$), 2.25 (m, $2H^1$), 1.54 (m, $3H^{10,11}$). ^{13}C NMR: 146.9 (C^7), 146.4 (C^4), 128.4 ($C^{5,9}$), 121.4 ($C^{6,8}$), 45.6 (C^2), 37.0 (C^3), 36.8 (C^1), 25.8 (C^{10}), 22.4 (C^{11}).

2.2.4. 9,9-Bis-(4-[(methylsulfonyl)oxy]phenyl)fluorene (2d)

This was synthesized from 9,9-bis-(4-hydroxyphenyl)fluorene. Yield: 2.71 g, 93 %, m.p. = 212–213 °C. ^1H NMR (25% DMSO, d_6, $CDCl_3$): 7.80 (d, $2H^{6,8}$, J_0 7.23), 7.29 (m, $6H^{5,9,10,11,12,13}$), 3.16 (s, $3H^3$). ^{13}C NMR: 148.4 (C^7), 146.5 (C^4),142.9 (C^{14}), 138.1 (C^1), 127.1 ($C^{5,9}$), 126.5 (C^{13}), 124.4 (C^{12}), 120.4 ($C^{6,8}$), 62.7 (C^2), 35.9 (C^3).

2.2.5. Oligo(4,4′-biphenylene-1,1-propylene) (3a)

The general procedure used for the synthesis of polymers **3a–d** is described in detail for **3a**. A 50 mL Schlenk tube was charged with $NiCl_2(PPh_3)_2$ (0.196 g, 0.3 mmol), PPh_3 (0,472 g, 1.8 mmol), Et_4NI (1.03 g, 4.5 mmol), Zn (1.378 g, 21.09 mmol) and **2a** (1.153 g, 3.0 mmol) and the mixture was kept under N_2 atmosphere. Dry THF (3.45 mL) was added via a syringe. The mixture was stirred for 5 min until it develop a deep red colour, then was heated at 67 °C for 48 h. The reaction mixture was poured into methanol (30 mL) and aqueous HCl (13 mL).The precipitate was collected by filtration, dissolved in $CHCl_3$ (4 mL) and poured into methanol (30 mL). The precipitate was collected by filtration and dried *in vacuo* (0.364 g; 63%). The solid was purified by two additional fractional reprecipitations of its chloroform solution in methanol (final yield: 25%). ^1H NMR ($CDCl_3$): 7.30 (d, $4H^{6,8}$, J_0 8.3), 7.48 (d, $4H^{6,9}$, J_0 8.3), 1.72 (s, $3H^1$). ^{13}C NMR: 149.9 (C^4), 138.6 (C^7), 127.6 ($C^{6,8}$), 127.0 ($C^{5,9}$), 43.0 (C^2), 31.2 (C^1).

2.2.6. Oligo(4,4′-biphenylene-1,1-hexafluorpropylene) (3b)

Yield: 38%. ^1H MNR ($CDCl_3$): 7.59 (d, $2H^{6,8}$, J_o 8.39), 7.59 (d, $2H^{5,9}$, J_0 8.39). ^{13}C NMR: 140.8 (C^4), 133.3 (C^7), 124.2 (c, $^1J_{C-F}$ 286.2) (C^1), 131.2 ($C^{5,9}$), 127.3 ($C^{6,8}$), 64.4 (m, $^2J_{C-F}$ 25.2) (C^2).

2.2.7. Oligo(4,4′-biphenylene-1,1-cyclohexylene) (3c)

Yield: 27%. ^1H NMR ($CDCl_3$): 7.39 (m, $4H^{5,6,8,9}$), 2.31 (m, $2H^1$), 1.55 (m, $3H^{10,11}$). ^{13}C NMR: 147.8 (C^4), 138.2 (C^7), 127.9 ($C^{5,9}$), 127.1 ($C^{6,8}$), 46.3 (C^2), 37.6 (C^1), 26.8 (C^{10}), 23.3 (C^{11}).

2.2.8. Oligo(4,4′-biphenylene-9,9-fluorenylene)(3d)

Yield: 21%. ^1H NMR ($CDCl_3$): 7.89 (d, $2H^{6,8}$, J_0 7.06), 7.50 (m, $6H^{5,9,10,11,12,13}$). ^{13}C NMR: 151.5 (C^4), 145.2 (C^7), 140.6 (C^{14}), 139.4 (C^{1}), 128.9 ($C^{5,9}$), 127.2 ($C^{6,8}$), 126.7 (C^{13}), 120.6 (C^{12}), 65.4 (C^{2}).

2.3. Measurements

Melting points reported are not corrected. ^{1}H NMR and ^{13}C NMR spectra were recorded on a Bruker ARX300 spectrometer on samples dissolved in $CDCl_3$. Gel permeation chromatography analyses were carried out on THF solutions at room temperature using a Waters model 600 equipped with a Waters 2487 UV detector set at 254 nm. Calibration of the instrument was done using polystyrene standards. Thermal analysis was carried out on a Perkin Elmer DSC7 under nitrogen flow. The scan rate was 10 °C/min. The thermal behaviour was observed on an optical polarizing microscope (Leitz, Model Ortolux) equipped with a hot stage (Mettler).

UV/vis spectra were obtained using a UV–visible GBC Cindra 20 spectrometer. The absorptions measurements were done either on dilute samples (<0.005 g/ml) or on thin films cast on quartz plates, which were placed at a 30° angle with respect to the incident beam. Emission spectra and steady-state fluorescence anisotropies (L-format, G factor-corrected) were obtained using an AMINCO 8100 spectrofluorimeter from dilute solutions or thin polymer films cast on quartz plates at 25 °C. The emission measurements were carried out either on dilute samples (less than 0.005 g/ml) or on thin films cast on quartz plates. The quartz plates were oriented 30° relative to the incident beam. Film specimens were drop-cast from a $CHCl_3$ solution on quartz substrates and dried at room temperature under reduced pressure.

2.4. Molecular modelling

Molecular modelling of the model compounds was carried out at the semi empirical level using the AM1 MO program implemented in the suite of programs Hyperchem (Version 7.5, Hypercube Inc.). Modelling was assumed to be carried out in the gas phase at 0 °K. Minimization operations were performed using the conjugate gradient method and halted by setting the gradient option at 0.01 kcal/mol. Conformational searches around the single bond that links the aromatic ring to the substituted methylene spacer were done by minimization of the energy function in conjunction with torsion angle restrains. The geometries found at minima were then minimized without restrains.

3. Results and discussion

Dimesylates **2a–d** were prepared in good yields from the corresponding diphenols **1a–d**. Compounds **3a–d** were synthesized by nickel-catalysed homocoupling reactions of the dimesylates in THF (Scheme 1). As noted before the synthesis of poly(*p*-arylenemethylene)s is hampered by solubility problems although the presence of nickel salts and Zn powder made it difficult ascertaining whether some of the material precipitated during the reaction. Since we found that all **3a–d** were very soluble in chloroform the materials were purified by three fractional reprecipitations of their chloroform solutions in methanol. The gel permeation analysis (Table 1) of the reprecipitated compounds showed that **3a–d** were oligomeric materials, i.e., **3a** and **3b** have degrees of polymerisation, DP; of about 10 while **3c** and **3d** have DP of 4, with monomodal and narrow distributions due to the reprecipitations from MeOH. Both **3c** and **3b** showed larger polydispersities due to the greater influence of the remnant end groups on the molecular weight of these short oligomers. It should be noted that light scattering techniques have indicated that GPC measurements using polystyrene standards underestimate 1.5 or 1.8 times the real average molecular weights in this class of materials [6,7]. As shown in Fig. 1 in the ^{1}H NMR of **3b**, the 3.15 ppm signal corresponding to residual mesylate end groups was very small and could not be used to calculate the DP. Similarly, the areas of the mesyl group signals in the 3.10–3.30 ppm range for **3a**, **3c** and **3d** were only less than 15% of the expected areas based on the GPC DP values. Possibly, mesyl groups were partially reduced during the coupling; it is also plausible that other mesyl groups could be hydrolysed during the harsh conditions of the workup. No signals corresponding to aromatic protons in the ortho positions with respect to the phenolic group were observed by NMR. Therefore, if hydrolysis occurs the phenolic groups should increase the oligomer solubility in MeOH/$CHCl_3$ mixture and preferentially remain in the soluble fractions. Moreover, the monomodal nature of the GPC traces precludes the presence of substantial amounts of cyclic oligomers.

The solubility of **3a–d** in common organic solvents like $CHCl_3$, THF or acetonitrile is very good. In particular,

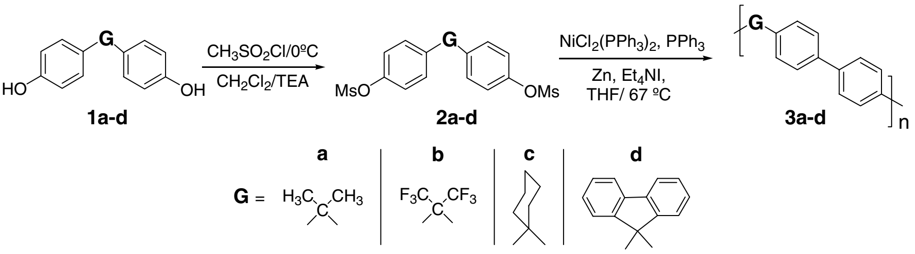

Scheme 1. Synthesis of monomers and oligomers.

Table 1
Physical properties of **3a–d**

	M_n/M_w[a]	PDI[b]	DPn[c]	EG[d]	SP/T_g[e]	S[g]
3a	1650/2050	1.24	9	14	165/140	0.6
3b	3100/3950	1.27	10	~3	202/186	1.0
3c	900/1300	1.44	4	7	125/n.o.[f]	0.8
3d	1400/1900	1.36	4	<2	299/275	0.8

[a] In $g \cdot mol^{-1}$ determined by GPC.
[b] Polydispersity index, M_n/M_w.
[c] Degree of polymerisation based on M_n.
[d] Residual mesylate end groups, % of the expected value based on GPC DP.
[e] Softening points observed visually by POM and glass transition temperatures determined by DSC, in °C.
[f] Not observed.
[g] Solubility in $CHCl_3$ per mole of repeating unit/L.

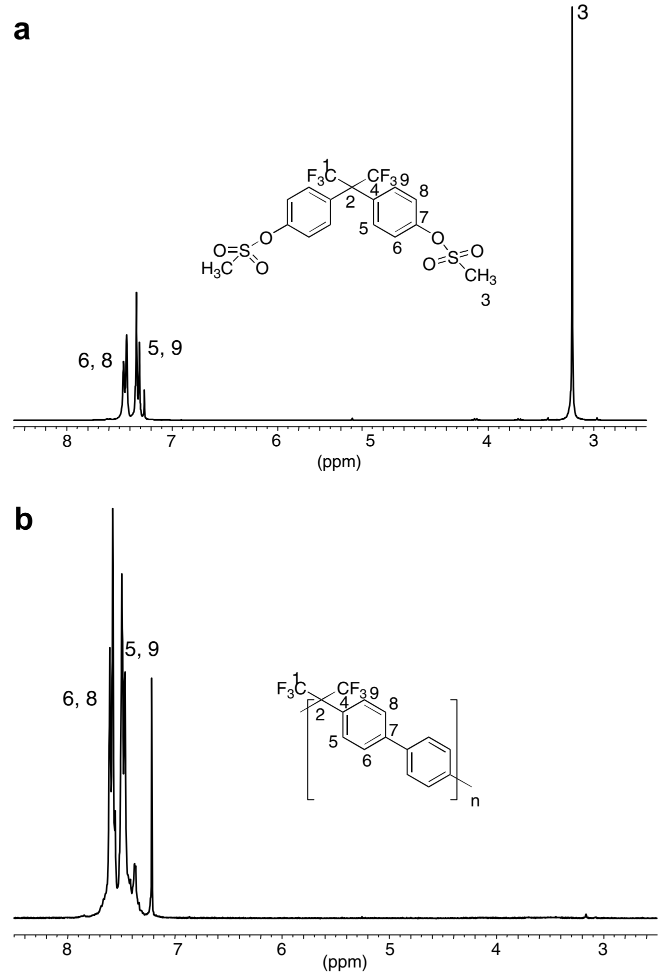

Fig. 1. ^{1}H NMR spectrum of **2b** and **3b** in $CDCl_3$.

$CHCl_3$ was the solvent of choice to prepare smooth transparent films suitable for optical measurements. The thermal properties of **3a–d** were examined at a temperature range between 50 and 300 °C using DSC and polarizing optical microscopy (POM). Compounds **3a–d** are amorphous in nature; no birefringence was detected by POM observations of films even after several annealing protocols and heating–cooling cycles around their softening temperatures. Besides, in most cases their DSC traces showed small glass transitions and no melting transitions were observed in all cases. Thus we observed that taking into account the differences in molecular weight neither the increase of the aliphatic moiety size from isopropylene to cyclohexylene nor the introduction of a fluorene moiety significantly improves solubility; while the perfluorinated derivative showed the highest processability.

The absorption and emission data of **3a–d** is summarized in Table 2. In principle, the optical properties of **3a–d** will be determined by intrachain as well as the interchain interactions between chromophores. As shown in Fig. 2a by the space-filling model of an octamer of **3a**, the individual polymer chains have a contorted open topology with the connector interrupting conjugation along the main chain. But it has been pointed out that the p-orbitals of the aromatic rings in 2,2-arylpropanes and related systems could overlap in apical cofacial conformations, also called butterfly conformations, leading to intrachain interaction between gem-chromophores [6,10,11]. This effect has been considered to be operative in 9,9-dioligophenylfluorenes [10]. We first evaluated the influence of the different spacers on gem-biphenyl conformations by molecular modelling. A conformational analysis performed at the AM1 semi empirical level on 2,2-dibiphenyl compounds **4a–d** (Fig. 2b) indicated that **4a**, **4b** and **4d** flip from one propeller conformation to another through low rotational barriers of 0.7, 1.2 and 2.5 kcal/mol by cooperative rotation of both gem-aromatic rings without adopting at any moment a cofacial conformation. Indeed, no butterfly conformation was detected in the case of the fluorenylene-based **4d**. The cyclohexylene-spaced **4c** showed a more complex pattern, the propeller conformations were at equilibrium with a higher energy perpendicular conformation while a butterfly-like conformation was detected at an energy maximum. The propeller and the perpendicular conformations lay at minima of different energy ($E_{perp} - E_{prop} = 0.45$ kcal/mol) while the butterfly conformation is

Table 2
UV and Photoluminescent data of **3a–d**

	$\lambda_{Abs,\ max}$[a] A/B (ε)[b]/C	$\lambda_{PL,\ max}$[c] A/B	Fwhm[e] A/B	SS[f] A/B	$\langle r \rangle$[g] A/B
3a	267/268 (1.6)/266	315/321	39/47	47/55	0.123/0.083
3b	265/263 (1.8)/263	303/325	45/55	40/62	0.020/0.028
3c	272/270 (1.7)/268	323/329	45/55	53/61	0.095/0.037
3d	267/272 (4.0)/272	313/329[d]	32/~59	41/57	0.004/0.103

[a] Absorption maxima (in nm), THF solution (A), $CHCl_3$ solution (B) and film (C).
[b] Molar extinction coefficient per mole of repeating unit, $10^4\ M^{-1}\ cm^{-1}$.
[c] Emission maxima (in nm), $CHCl_3$ solution (A) and film (B), $\lambda_{exc} = \lambda_{Abs,\ max}$.
[d] Excimer band at 417 nm.
[e] Full width at half-maximum of the fluorescence bands (in nm) in solution (A) and film (B).
[f] Stokes shifts in solution (A) and film (B).
[g] Steady-state emission anisotropy ($\lambda_{exc} = 280$ nm).

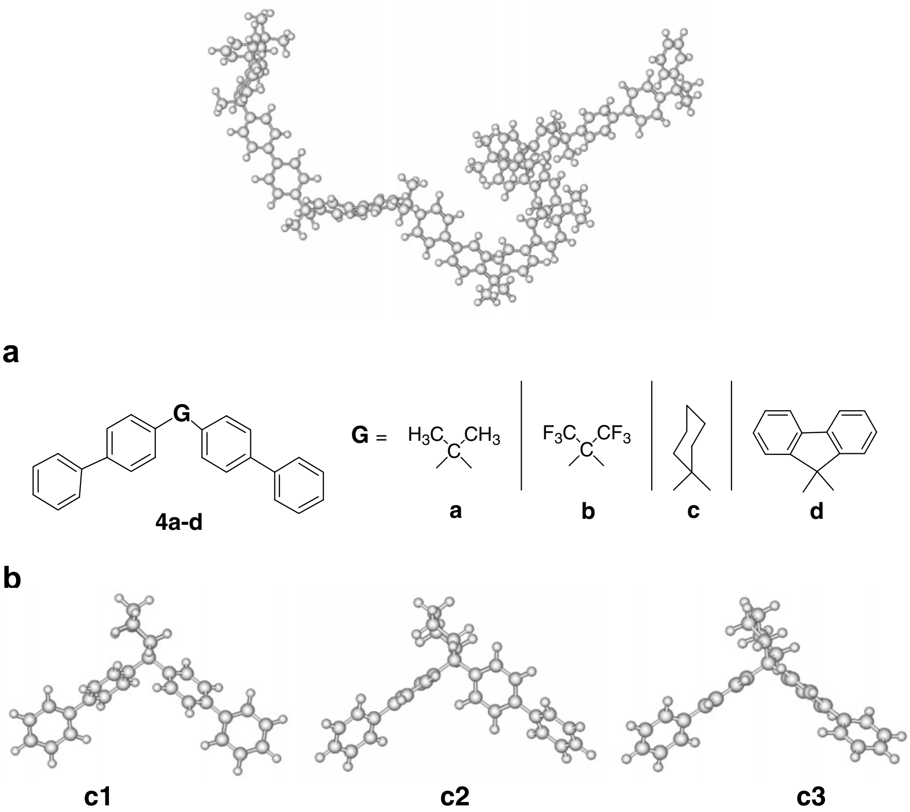

Fig. 2. (a) AM1 molecular model of an octamer of **3a**. (b) Molecular structure of compounds **4a**–**d**. (c1) Propeller conformation of **4c**. (c2) Perpendicular conformation of **4c**. (c3) Butterfly conformation of **4c**.

at the maximum between two propeller conformations with rotational barrier of 0.8 kcal/mol. Thus, gem-biphenyl interactions, if any, can only be expected in **4c**.

The absorption spectrum of 2,2-diphenylpropane, which has the phenyl groups arranged in a propeller conformation, consists of an intense aromatic conjugation band (K band) in the high-energy zone near 200 nm and a weaker band around 270 nm. An additional third band, which is considered to be the spectral signature of homoconjugative interactions between gem-diphenyls, has been observed around 230 nm in 7,7-diphenylnorbornane derivatives where the aryl rings are forced to adopt a cofacial disposition with a ring-flip barrier of 15 kcal/mol [12,13]. However, this third band appeared in 7,7-dibiphenylnorbornane as a shoulder of the π–π^* band at ca. 340 nm and therefore homoconjugative interactions could be difficult to identify since their only optical manifestation would be a bathochromic shift of the π–π^* band [13]. In our case, both 2,2-diphenylpropane and 4,4′-ditertbutylbiphenyl, **5**, can be considered as model compounds of **3a**–**d** to help addressing the question whether the gem-biphenyls interact along the chain or are effectively isolated by the sp^3-carbon atom. Fig. 3A shows that the film spectra of **3a**–**d** are all qualitatively related to the spectrum of 2,2-diphenylpropane. Hence they exhibit only two bands though the π–π^* bands of **3a**–**d** are stronger than that of 2,2-diphenylpropane. The absorption spectrum of perfluoropropylene-spaced **3b**, while consistent with the spectra shown by the other members of this series, has no resemblance with the one already reported which shows a peculiar intense and well resolved vibronic structure around 250 nm and a π–π^* band extending up to 340 nm [7]. On the contrary, the absorption spectrum of fluorene-spaced **3d** concords with the one previously reported [6]. It shows a broader band and a greater extinction coefficient than **3a–c** due to the presence of two chromophores, biphenyl and fluorene, in the repeating units. Fig. 3B shows that the absorption maxima in THF solution of the low energy band are about 4–13 nm red-shifted in comparison with that of the isolated biphenyl **5** ($\lambda_{\max} = 259$ nm, in THF). The small bathochromic shift increases with the donor character of the spacer. Moreover, the cyclohexylene-spaced **3c** shows no significant red shift either in solution or film with respect to the propylene-spaced **3a**. Therefore, the small differences observed in gem-diarylpropylenes and related systems between model compounds and macromolecular absorption maxima can be assigned to substitution effects without invoking homoconjugative effects.

The absorption and PL spectra in chloroform solution and film of **3a**–**d** are shown in Fig. 4. As was observed with absorption, an increase in the electron-donating properties of the spacer causes a small bathochromic shift in the emission of **3a**–**c** in solution. The planarization of the first excited state structure of the biphenyl chromophore results in moderate Stokes shifts of 40–50 nm similar to that observed in biphenyl. The emission band of **3d** with a nar-

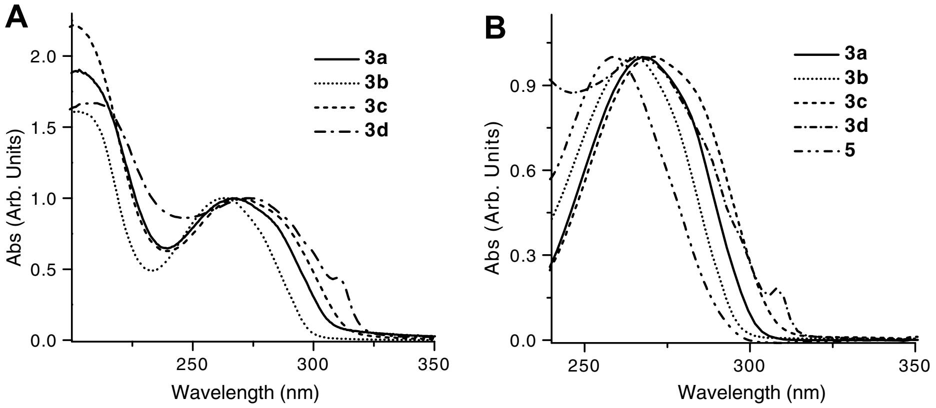

Fig. 3. (A) Absorption spectra of **3a**–**d** films. (B) Absorption spectra of THF solutions of **3a**–**d** and **5**.

row full width at half-maximum, fwhm, and little tailing features that of the fluorene group and more than doubles the emission intensity of **3a–c**. Thus, the fluorescence measured in **3d** is emitted predominantly from the fluorene moieties due to their higher quantum yield while the biphenylene emission is either masked or decreased by energy transfer to fluorene groups. In dilute solution, excitation migration can only occur within each oligomeric chain which can be considered as a small cluster with a number average of either four chromophores in **3c** or 8–10 chromophores in **3a**, **3b** and **3d**. Fluorescence depolarisation measurements are frequently used to study excitation energy transfer in multichromophoric assemblies [14]. We then performed steady-state fluorescence anisotropy measurements in solution and films and results are shown in Table 2. Though anisotropy values near zero could be expected in solution for these medium size molecules due to long exciton lifetimes of biphenyl and fluorene and to rotational depolarisation and energy transfer, all oligomers but **3d** showed larger values. So no information

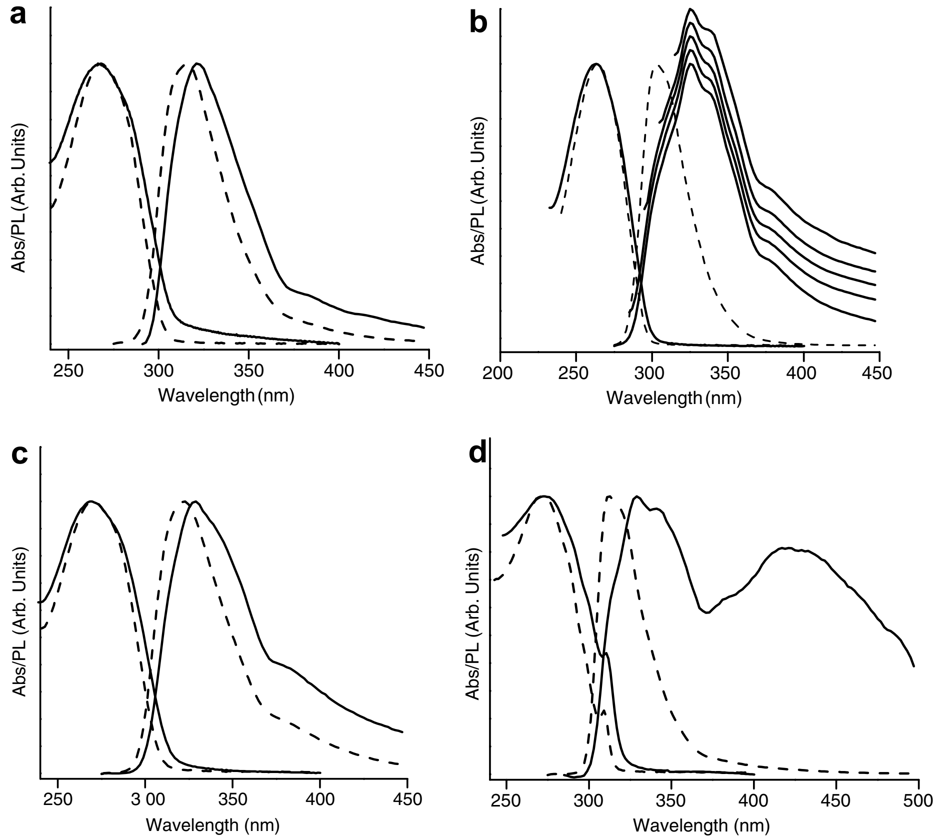

Fig. 4. Normalized absorption and emission spectra of $CHCl_3$ solutions (dashed curves) and films (solid curves) of **3a**–**d**. The PL spectra were obtained by excitation at 270 nm. The spectra of **3b** shows also the PL spectra obtained by excitation at 280, 290, 300, 310 nm.

can be obtained from the almost complete depolarisation of **3d**. On the other hand, it can be argued that an enhancement of the transfer rate between the gem-biphenyls due to Dexter mechanism should occur if homoconjugation takes place in **3c**. But despite its smaller size **3c** showed an anisotropy value comparable to that of **3a**. Consequently, it can be concluded from the absorption and emission behaviour of **3a–d** that the spacer effectively isolates the gem-biphenyls.

The comparison between the optical behaviour in solution and neat films permits evaluating the influence of the spacers on interchain interactions and solid-state packing effects. Thus, **3a–d** show in films a solution-like absorption spectra with only an additional small inhomogeneous broadening indicating that in the amorphous state chromophore planarization is not enhanced by ground-state interactions between chains. However, all emission bands are broader and have red-shifted maxima in the condensed phase. In addition, solid-state emissions are much more dependent on the spacer nature than absorption. While both **3a** and **3c** show comparable emission spectra irrespective of the size of the nonpolar spacer, the higher fwhm and tailing of the emission band in the perfluorinated **3b** arise from its higher chain rigidity and stronger interactions between chains. However, the band broadening could also be due to emission from ground-state aggregates whose presence cannot be easily ruled out by inspection of the absorption spectra because the tail of the single chromophore absorption can blur the distinct absorption band of the aggregates [15]. Fig. 4 also shows the results of the red-edge excitation experiments in a neat film of **3b**. The similarity of the emission spectra obtained by exciting at different energies from 270 to 310 nm on the red-edge of the absorption spectrum indicates that fluorescence is emitted by the same species, i.e.,: the isolated excited chromophores. Analogous data was obtained in similar experiments carried out with **3a**, **3c** and **3d**. Therefore, no aggregate formation was detected in **3a–d**. Then, the large broad band peaking at 417 nm that appeared in addition to the 329 nm emission from single chromophoric units in the bichromophoric system **3d** may be attributed to fluorene excimers. The fluorene groups in **3d** are placed in the periphery of the polymer chain and consequently are accessible for interaction. Indeed, it has been observed that the fluorene excimer emits in solution at 387 nm with a shoulder at 411 nm [16] but in solid-state larger Stokes shifts should be expected. The steady-state emission anisotropies of **3a–d** measured in films where excitation energy homotransfer is the only possible source of emission depolarisation because reorientation of chromophores is halted indicated that bulk exciton mobilities in these disordered assemblies are high despite the moderate Stokes shifts. The residual anisotropy is defined by the ratio of the excitation transfer rate to the emission decay rate. Although **3a–c** share the same chromophore, a longer decay rate is expected for **3b** with the more rigid perfluorinated spacer that would provide less non-radiative decay channels leading to a lower anisotropy. On the other hand, the higher anisotropy value of **3d** could be due to the shorter lifetime of fluorene emission.

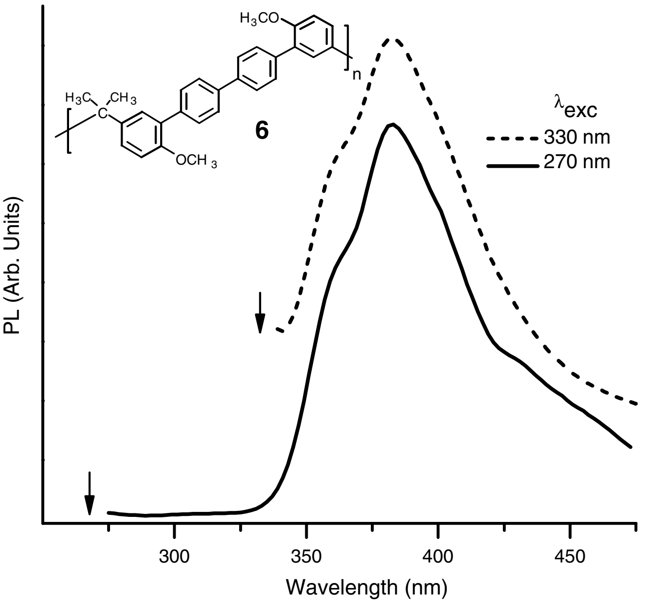

Fig. 5. Normalized PL spectra of the blend of **3a** and **6** excited at 270 nm and 330 nm.

We also found that **3a** is a highly efficient donor as well. Thus, a film of a 1:1 (wt./wt.) blend of **3a** and the quaterphenylene-based polymer **6** was made. Polymer **6** has a $\lambda_{\mathrm{Abs,max}} =$ 306 nm, a $\lambda_{\mathrm{PL,max}} = 387$ nm and showed in neat films a $\langle r \rangle_{\mathrm{neat\ film}} = 0.271$ [17]. When it was excited at 330 nm in the blend its emission spectrum is identical to that of the neat film although its anisotropy is somewhat lower, $\langle r \rangle_{\mathrm{blend}} = 0.190$. **3a** and **6** show good spectral overlap and when the blend was excited at $\lambda_{\mathrm{Abs,max}} = 270$ nm, i.e., the absorption maxima of biphenylene-based polymer, no emission from the biphenylene chromophore was detected at 330 nm. Instead, as shown in Fig. 5 a depolarised emission spectra of **6** ($\langle r \rangle_{\mathrm{blend}} = 0.050$) was obtained, indicating quantitative excitation energy transfer from the biphenylene to the quaterphenylene chromophore.

4. Conclusions

The poly(*p*-biphenylene methylene)s prepared by homocoupling have low polydispersity indexes, few residual end groups and good solubilities. Processability suffered when cyclohexylidene or fluorene spacers were introduced. They are amorphous UV-absorbers and emitters with good film-forming properties. The increase in size or polarity of the isopropylidene spacer does not bring major changes in their optical properties while the introduction of a fluorene spacer substantially modifies the optical response. It was concluded from the absorption and emission behaviour of **3a–d** that the spacer effectively isolates the gem-biphenyls and the small differences observed between model compound and macromolecular absorption maxima can be assigned to substitution effects without invoking homoconjugative effects. No aggregate formation was detected indicating that their contorted chain conformations hinder interactions between the biphenylene chromophores. However, the fluorene units placed in the periphery of **3d** form fluorene excimers. Notwithstanding the moderate Stokes shifts the bulk exciton mobilities by excitation migration in these disordered assemblies are high. We also found that **3a** is a highly efficient donor for energy transfer.

Acknowledgements

Financial support was provided in parts by ANPCyT and SGCyT-UNS, Argentina. P.G. D.R. and M.F.A. thank CONICET for fellowships.

References

[1] (a) A. Greiner, Polym. Adv. Technol. 9 (1998) 371;
(b) L. Akcelrud, Prog. Polym. Sci. 28 (2003) 875.

[2] D. Steiger, T. Tervoort, C. Weder, P. Smith, Macromol. Rapid Commun. 21 (2000) 405.

[3] A. Greiner, S. Mang, O. Schäfer, P. Simon, Acta Polym. 48 (1997) 1.

[4] C. Schmidt, V. Stümpflen, J.H. Wendorff, A. Hasenhind, W. Gronski, M. Ishaque, A. Greiner, Acta Polym. 49 (1998) 232.

[5] Y.S. Son, H.Y. Park, Y.C. Lim, K.G. Choi, K.C. Lee, G.B. Park, C.J. Lee, D.J. Moon, J.I. Han, Y.B. Kim, S.C. Nam, Thin Solid Films 513 (2006) 258.

[6] M. Beinhoff, L.D. Bozano, J. Campbell Scott, K.R. Carter, Macromolecules 38 (2005) 4147.

[7] P.A. Havelka-Rivard, K. Nagai, B.D. Freeman, V.V. Sheares, Macromolecules 32 (1999) 6418.

[8] F. Huang, Y.-H. Niu, M.S. Liu, X.-H. Zhou, Y.-Q. Tian, A.K.-Y. Jen, Appl. Phys. Lett. 89 (2006) 81104.

[9] M.L. Venanzi, J. Chem. Soc. (1958) 719.

[10] R. Faber, A. Stasko, O. Nuyken, Macromol. Chem. Phys. 201 (2000) 2257.

[11] C.A. van Walree, M.R. Roest, W. Schuddeboom, L.W. Jenneskens, J.W. Verhoeven, J.M. Warmen, H. Kooijman, A.L. Spek, J. Am. Chem. Soc. 118 (1996) 8395.

[12] A. Garcia Martinez, J. Osio Barcina, A. Fresno Cerezo, R. Gutiérrez Rivas, J. Am. Chem. Soc. 120 (1998) 673.

[13] A. Garcia Martinez, J. Osio Barcina, A. Fresno Cerezo, A-D. Schlüter, J. Frahn, Adv. Mater. 11 (1999) 27.

[14] H.-J. Egelhaaf, J. Gierschner, D. Oelkrug, Synth. Met. 83 (1996) 221.

[15] I.D.W. Samuel, G. Rumbles, R.H. Friend, in: N.S. Sariciftci (Ed.), Primary Photoexcitations in Conjugated Polymers, World Scientific Publishing Co. Pte. Ltd., London, 1997, pp. 140–169.

[16] F.M. Winnik, Macromolecules 22 (1989) 734.

[17] $M_n/M_w = 4400$ Da/7500 Da, $T_g = 161$ °C. P.G. Del Rosso, M.F. Almassio, R.O. Garay, to be published.